THIS DOCUMENT IS PROTECTED BY U.S. COPYRIGHT
It may not be reproduced, stored in a retrieval system, distributed or transmitted, in whole or in part, in any form or by any means.
Downloaded from SAE International by Argonne National Laboratory, Copyright 2011 SAE International
Monday, November 07, 2011 12:11:32 PM

SAE International

Numerical and Optical Evolution of Gaseous Jets in Direct Injection Hydrogen Engines

2011-01-0675
Published
04/12/2011

Riccardo Scarcelli, Thomas Wallner and Nicholas Matthias
Argonne National Laboratory

Victor Salazar and Sebastian Kaiser
Sandia National Laboratories

Copyright © 2011 SAE International

doi:10.4271/2011-01-0675

ABSTRACT

This paper performs a parametric analysis of the influence of numerical grid resolution and turbulence model on jet penetration and mixture formation in a DI-H2 ICE. The cylinder geometry is typical of passenger-car sized spark-ignited engines, with a centrally located single-hole injector nozzle. The simulation includes the intake and exhaust port geometry, in order to account for the actual flow field within the cylinder when injection of hydrogen starts. A reduced geometry is then used to focus on the mixture formation process. The numerically predicted hydrogen mole-fraction fields are compared to experimental data from quantitative laser-based imaging in a corresponding optically accessible engine.

In general, the results show that with proper mesh and turbulence settings, remarkable agreement between numerical and experimental data in terms of fuel jet evolution and mixture formation can be achieved. The grid resolution is found to have significant influence on the jet penetration, and almost no effect on the fuel dispersion. In order to improve the prediction of local values of air/fuel ratio, tuning of the turbulence model is performed. Results show that the turbulence model affects fuel dispersion but not jet penetration.

INTRODUCTION

Hydrogen-fueled internal combustion engines (H2 ICES) have been studied for several decades, resulting in extensive literature [1,2,3]. Hydrogen is a promising fuel to reduce overall carbon dioxide emissions. Even though the higher efficiency and lower emissions of hydrogen in fuel cell applications have relegated the interest in H2 ICES mainly to a bridging technology toward a future large-scale hydrogen infrastructure, the interest in H2 ICES is still alive due to the significant potential in reducing the efficiency -NOX trade-off affecting most of the conventional engines. The U.S. Department of Energy has set challenging goals for H2 ICES: 45% brake thermal efficiency and NOX emissions of 0.07 g/mile, together with a power density comparable with gasoline engines at a mass-production cost of 30 $/kW [4].

In order to meet these targets, Argonne National Laboratory has been researching advanced mixture formation and combustion concepts, including in-cylinder emission-reduction measures [5,6,7,8,9]. Direct Injection (DI) has proven to be a promising approach to help meeting the above-mentioned objectives [10] since, compared to port fuel injection (PFI), it allows higher specific power. DI also avoids the risk of backfiring, thus increasing the level of safety and widening the range of operating conditions. Furthermore, due to the fast air-fuel mixing and wide flammability range of hydrogen, fueling strategies such as late injection provide the opportunity of reducing compression work and increasing engine efficiency. DI-H2 ICES are already able to achieve high peak-levels of BTE [11,12]. The challenge consists in the proper control of both geometrical and operational injection parameters, which need to be correctly set in order to achieve the proper mixture stratification in the combustion chamber at the spark timing. Therefore, research on DI-H2 engines has been focusing on advanced injector design and injection strategies to improve the engine efficiency while reducing exhaust emissions.

THIS DOCUMENT IS PROTECTED BY U.S. COPYRIGHT
It may not be reproduced, stored in a retrieval system, distributed or transmitted, in whole or in part, in any form or by any means.
Downloaded from SAE International by Argonne National Laboratory, Copyright 2011 SAE International
Monday, November 07, 2011 12:11:32 PM

In this scenario, the development of a numerical approach can provide important input to the experimental testing. A numerical approach cannot ever replace real engine testing. The significant potential of a modeling approach lies in exploring new settings and geometries with the final goal to improve the experimental result. By means of rigorously validated CFD, innovative technological solutions can be numerically tested within hours and manufactured in case of positive response, thus drastically reducing the related production cost and time. Accordingly, effort has to be put into ensuring reliability and accuracy of computational codes, which can be assessed by means of validation against experimental data.

A three-dimensional computational fluid-dynamic model (3D-CFD) of a DI-H2 ICE has been developed at Argonne National Laboratory. Simulations performed in this paper use the commercial code Fluent (v6.3.35) and Reynolds-Averaged Navier Stokes (RANS) approach to model in-cylinder turbulence. Although RANS introduces a higher level of approximation in describing turbulence scales compared to large eddy simulation (LES) or direct numerical simulation (DNS), the first is computationally more affordable. Moreover, the RANS approach has been demonstrated to successfully predict mixture measurements in other H2 ICES [13,14].

The high level of detail of modern numerical simulations requires comparable detail in experimental data for a proper validation. In addition to global data on engine performance like brake thermal efficiency and exhaust emissions, direct insight into the mixture formation and combustion can be gained by laser-based measurements in optically accessible engines. Previous work at Sandia National Laboratories used planar laser-induced fluorescence (PLIF) and particle image velocimetry (PIV) to examine the air/fuel mixing after injection from multi-hole nozzles [15,16]. Even though practical implementations of DI in H2 ICES are likely to employ such multi-hole nozzles for faster mixing, the geometric complexity and jet-jet interaction make the interpretation of the experimental data challenging. Therefore, a subsequent optical study was based on a single-hole nozzle [17], which also provides a more canonical case for the current simulation validation.

Preliminary results of this joint experimental and numerical work are reported in references [18,19]. The current work expands the code validation process with a parametric study of the influence of computational grid size and turbulence model settings on the evolution of the hydrogen supersonic jet during the entire compression stroke. In the experiments, the measurement of fuel concentrations was improved by reducing the typical error in converting the florescence of the acetone tracer into actual hydrogen mole-fraction, and provided a better term of comparison for the numerical investigations. Still, differences between numerical and experimental results persisted in terms of fuel concentration. Accordingly, the above-mentioned parametric study is introduced to provide a comprehensive numerical analysis, with the goal to improve the quality of numerical data and to assess its reliability. The resulting validated numerical approach is envisioned to guide future experimental optimization of main parameters (injection timing and nozzle configuration) and performance in gaseous (H2, CNG, etc.) DI engines.

EXPERIMENT

OPTICAL ENGINE

The optical engine at Sandia National Laboratories is a passenger-car sized, four-stroke single-cylinder research engine, adapted to operate with hydrogen. Large transparent segments make the engine optically accessible for laser-based measurements. Schematics of the relevant optical and mechanical components are shown in Figure 1. The engine has a four-valve head with a pent-roof combustion chamber. The piston is flat-topped. The intake system consists of two intake ports, one for each valve, both straight and parallel to each other forming an angle of 40° with respect to the fire deck (horizontal). For this study, a full-length fused-silica liner is used, so that the entire volume swept by the piston is optically accessible, but not the pent-roof [17].

The main engine geometrical and operating parameters are given in Table 1. The crank-angle convention used in this paper assigns 0°CA to compression TDC. Thus, crank-angles during the compression stroke are negative. Hydrogen is supplied at 100 bar injection pressure, directly into the combustion chamber via a solenoid injector from Westport Inc. As shown in Figure 1a, the injector nozzle has a single orifice with a diameter of 1.46 mm and a 50° angle with respect to the injector axis. Figure 1b shows the injector, centrally located between the four valves, and the nozzle direction, aiming at the intake squish region (between the two valves) and downward. The jet is aligned with the mirror-symmetry plane of the combustion chamber. All data reported here correspond to this central symmetry plane.

Since the present study is focused on the mixture-formation process prior to ignition, fired engine operation is not necessary. The engine is motored at a constant speed of 1500 RPM, and nitrogen is supplied as a bulk gas (but treated as air in calculations of the equivalence ratio). The pressure in the surge tank upstream of the intake runner is kept at 1 bar and typical intake temperatures just upstream of the engine head are around 36°C.

THIS DOCUMENT IS PROTECTED BY U.S. COPYRIGHT
It may not be reproduced, stored in a retrieval system, distributed or transmitted, in whole or in part, in any form or by any means.
Downloaded from SAE International by Argonne National Laboratory, Copyright 2011 SAE International
Monday, November 07, 2011 12:11:32 PM

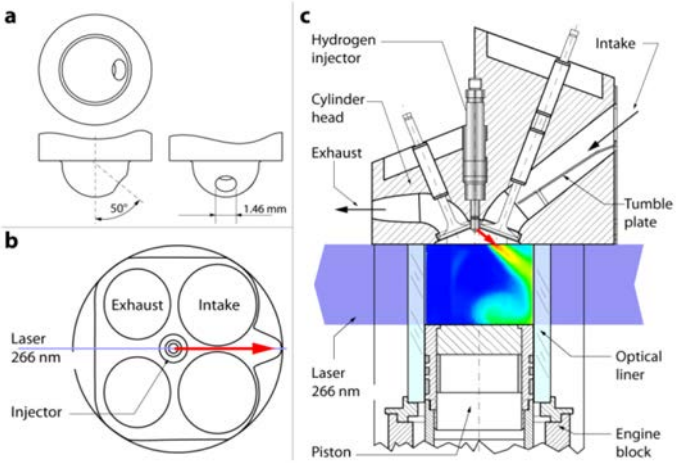

Figure 1. Schematics of engine hardware, (a) Geometry of the single-hole injector nozzle, (b) location and targeting of the injector with respect to the combustion chamber, (c) upper engine with measurement plane.

Table 1. Optical engine specifications and main operating parameters

Bore / Stroke / Displacement	92 mm / 85 mm / 565 cm^3
Compression ratio	11
Speed	1500 rpm
Intake pressure / Temperature	1 bar / 36°C
Intake valve Closing	-140°CA
Nominal / Actual SOI	-140°CA / -137°CA
H2 Injection Pressure	100 bar
Injection Duration	17.5°CA

To obtain a global equivalence ratio of 0.25 (λ = 4.0) or a hydrogen mole-fraction of 0.095, hydrogen fuel is injected for 17.5°CA at 100 bar. In fired operation, at typical efficiencies, this fuel concentration represents a low-load condition with about 2.5 bar IMEP. The mean fuel flow is measured far upstream of the injector with a thermal mass-flow meter (Brooks SLA5860). The fuel injection starts shortly after the intake-valve closure (SOI = −140°CA) to yield the maximum observable time span during the compression stroke. With the injection command issued at −140°CA, flow from the nozzle starts at −137°CA and ends at −119.5°CA.

PLIF MEASUREMENTS

Planar laser-induced fluorescence (PLIF) of gaseous acetone as a fuel tracer is adapted to obtain quantitative images of the hydrogen mole-fraction in the operating engine. The imaging technique is described in detail in previous work [20] and only briefly discussed here. Gaseous acetone is seeded as a tracer into the hydrogen fuel by a high-pressure bubbler. At 100 bar pressure and room temperature, a volume concentration of 0.33% can be reached. For current purposes, differential diffusion of tracer and fuel is estimated to be insignificant due to the large spatial structures examined here and the high Reynolds number of the post-injection flow. A quadrupled Nd:YAG at 266 run laser excites acetone fluorescence. Laser energies of about 100 mJ/pulse and a sheet-forming lens combination with f = 1500 mm are used. Anf = 50 mm, f/1.2 camera lens with an achromatic f = 500 mm "close-up" lens focuses the visible part of the acetone fluorescence onto an unintensified, back-illuminated CCD camera. Rejection of elastically scattered UV laser-slight by the glass lenses is sufficiently good to omit a long-pass filter.

Standard background and flat-field corrections are performed to quantify the measurements. For the latter, a nearly homogeneous charge is prepared by DI during the intake stroke. Distortion due to the curved liner is corrected. Inhomogeneities in the temperature field, induced by mixing of cold hydrogen and hot bulk gas, are accounted for based on known spectroscopic properties of the tracer [21,22] and on the assumption of adiabatic mixing between fuel and bulk gas [23,24,25]. The overall typical maximum error in the ensemble-mean equivalence-ratio fields is estimated to be 25%. Small regions in the images, in particular for early crank angles, may have larger errors because of local window fouling and signal reflections. 90 images of the hydrogen mole-fraction are collected at each crank-angle. The resulting sequence of phase-locked mean images has already been reported in a previous publication [17].

NUMERICAL SIMULATION

CFD simulations of direct injection of hydrogen and mixture formation are performed using the commercial CFD solver Fluent (version 6.3.35). The Gambit software is used as pre-processor to generate the computational grids.

COMPUTATIONAL GRIDS

The overall strategy of grid generation and numerical simulation followed in this study has been documented before [18,19] and can be briefly summarized as follows :

- A computational grid for the full engine geometry (including valves and ducts) is used to compute the in-cylinder flow-field during the gas-exchange phase, prior to fuel injection.
- A computational grid of the geometry reduced to the combustion chamber only (including the nozzle geometry) is used to simulate the direct injection and mixture formation processes.
- The flow field, state variables, and turbulence-model parameters calculated from the gas-exchange phase (step 1) are set as initial conditions for the subsequent simulation of direct injection and mixture formation (step 2).

By this approach, for a specific operating condition (engine speed and load), different injector geometries (number of

THIS DOCUMENT IS PROTECTED BY U.S. COPYRIGHT
It may not be reproduced, stored in a retrieval system, distributed or transmitted, in whole or in part, in any form or by any means.
Downloaded from SAE International by Argonne National Laboratory, Copyright 2011 SAE International
Monday, November 07, 2011 12:11:32 PM

nozzles, nozzle diameter, direction and location) and injection strategies (injection pressure and timing) can be evaluated on the reduced grid without the need to re-calculate the pre-injection flow-field. Furthermore, the high-pressure DI process with its transient supersonic jet requires higher grid resolution than the simulation of the gas exchange. Accordingly, the two processes are separated and two different grids are used.

The full-geometry grid consists of about 400,000 cells at BDC, mainly as a tetrahedral mesh (deforming zone), with the exception of the upper valve and piston zones (layering zone), where a hexahedral- or wedge-based mesh allows for the motion of the valve and piston surfaces. At valve opening times, sliding interfaces are created in the mesh to allow for valve motion. The simulation of the gas exchange starts at exhaust valve opening (EVO). Multi-cycle simulations were performed as well, but for the non-fired operation considered here there was no significant difference to initiation at stagnation conditions. Therefore, only the first simulation cycle is analyzed here. The initial pressure and temperature in the cylinder, intake, and exhaust are set on the basis of the experimental data. Pressure boundary-conditions at the ends of intake and exhaust ducts are measured in the optical engine by means of high-speed pressure transducers. The in-cylinder bulk-gas temperature during intake, which is not directly measured, is calculated from the intake and exhaust temperature by adiabatic compression/expansion. Intake and exhaust-valve lifts are taken from measurements. During the gas-exchange phase, a constant time-step of 0.5°CA is maintained. Simulation of the gas-exchange process ends at intake-valve closing (IVC). Velocity, state variables, and computational quantities like turbulence parameters are stored and interpolated onto the reduced-geometry grid as initial conditions for the subsequent simulation of the compression stroke.

The reduced-geometry mesh, on which injection and mixture formation are calculated, has similar topology as the full-geometry mesh used for the gas-exchange phase. A layering zone is still present to accommodate piston motion. The grid resolution is significantly increased to correctly simulate the hydrogen supersonic jet and the fast mixing with the bulk gas, nevertheless the simulation is still affordable in terms of computational time, due to multi-core parallel computing and considering that only the compression stroke (from IVC to TDC, resulting in 140°CA) is simulated on this grid.

The influence of grid size on numerical results on gaseous jet penetration and diffusion, especially in constant volume domains, has been extensively studied in terms of near-nozzle as well as overall resolution. Abraham [26] pointed out the minimum requirement for the number of computational cells (from 4 to 8) along the nozzle diameter. Andreassi et al. showed the influence of the overall mesh resolution on the jet penetration [27] and of the near-wall treatment on the jet impingement on the cylinder walls [28]. The present work, however, evaluates the gaseous injection and mixture formation process in a real engine and compares modeling and experiments along the entire compression stroke. In a preliminary work [18], the authors utilized coarse (250,000 cells at BDC) and fine (over 1,000,000 cells at BDC) meshes and found significant influence of the grid density on the numerical results, with particular regard to jet penetration and interaction with cylinder walls. A subsequent study [19] showed that by a 1,400,000 cells (at BDC) computational mesh it is possible to correctly predict the supersonic jet penetration and overall evolution. This paper reports a sensitivity analysis of the influence of the grid resolution on the numerical results and compares the results to the optical data.

DIRECT INJECTION OF HYDROGEN

Data in literature on numerical simulation of high-pressure hydrogen jets, with particular regard to in-cylinder domains, are scarce compared to liquid fuels in gasoline or diesel engines. Still, results from different gaseous fuels (CNG, methane, propane, even air) and different applications are useful in order to highlight important physics of gaseous jets and critical issues in numerical methods used to describe them.

As far as research on gaseous DI engines is concerned, in some cases injection models have been implemented into the available numerical codes in order to bypass their limitations or improve their accuracy. Hessel et al. [29] modified the KIVA-3V code to include a gaseous sphere injection model, in analogy with the liquid droplets injection model already provided in KIVA. Whitesides et al. [30] have applied this method to model the under-expanded jets in high-pressure DI-H2 ICES. Using this methodology, it is possible to employ relatively coarse computational grids and avoid the need to resolve the injector nozzle, which requires a higher level of geometric detail. Hybrid approaches have also been used for CNG [31] and H2 [32] DI ICES, with the aim to calculate the jet properties in the supersonic region (also called Mach disk) and avoid small cell sizes in the near-nozzle domain. Although these efforts have resulted in good agreement with experimental data in terms of jet penetration, in some cases no information on the spatial distribution of air entrainment in the jet has been provided or the numerical results have been not validated in terms of fuel concentration. The comparison of numerical data on mixture formation with PLIF optical data has been the main focus of some research groups [13,14,33] that have followed an engineering approach and used commercial codes to simulate high pressure gaseous jets in DI engines.

For the present simulations, the hydrogen mass flux through the nozzle is calculated by means of the measured mean mass-flow rate, injection duration, and nozzle diameter, and

THIS DOCUMENT IS PROTECTED BY U.S. COPYRIGHT
It may not be reproduced, stored in a retrieval system, distributed or transmitted, in whole or in part, in any form or by any means.
Downloaded from SAE International by Argonne National Laboratory, Copyright 2011 SAE International
Monday, November 07, 2011 12:11:32 PM

is set as the mass-flow inlet boundary condition for the injecting surface. Experimentally, at 1500 RPM a delay of about 3°CA is observed between the injector opening command and the actual start of injection (SOI). Accordingly, for a nominal value of SOI = −140°CA, the mass flux through the nozzle begins at −137°CA. The total injection duration is 17.5°CA. The actual injector-needle lift profile is not experimentally measured; instead, the fuel-mass flux is assumed to be constant with a linear 1°CA ramp-up and 1°CA ramp-down as shown in Figure 2. The resulting total mass injected per cycle (proportional to the area under the trace in Figure 2), corresponds to that calculated from the experimental multi-cycle mean hydrogen flow rate (3.46 mg/cycle). At the end of injection (EOI), the boundary condition for the injecting surface is changed from mass-flow inlet to wall. During the compression stroke a 0.5°CA time-step is used, with the exception of injection ramp-up and -down, where the rapid variation of mass flux requires a smaller (0.1°CA) time-step for stable calculations.

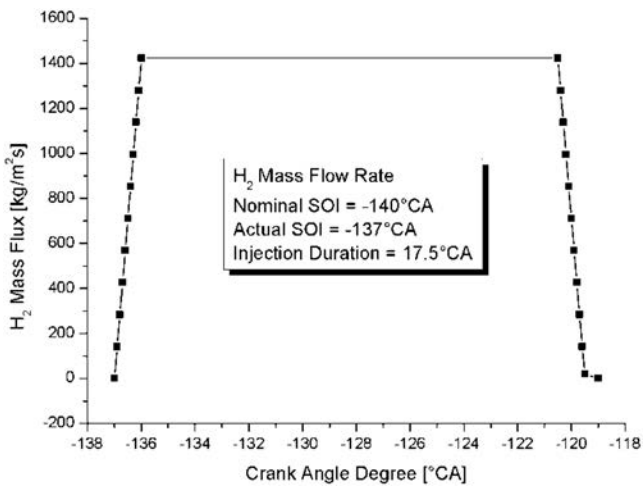

Figure 2. H2 mass flux through the injector nozzle

TURBULENCE MODEL

The Reynolds-Averaged Navier Stokes approach (RANS) is commonly used in engineering applications, due to the choice of modeling all the scales of turbulence, thus avoiding high resolution computational grids and providing numerical results in a reasonable computational time. Recently, academia and research environments have been increasingly dealing with more accurate LES and DNS approaches, which nevertheless are not computationally affordable yet for engine applications, characterized by either large computational domains and high Reynolds numbers. These two main issues significantly increase the grid resolution and consequently the computational time.

This study follows a RANS approach combined with a k-ε model to describe in-cylinder turbulence. All the formulations of the k-ε model provided by Fluent (k-ε standard, k-ε RNG, k-ε realizable) have been previously tested and shown only slight differences in the numerical results. So far, the k-ε RNG has been chosen by the authors [18,19] based on the present application and due to well-known limitations of k-ε standard. In fact, the k-ε RNG accounts for the effects of smaller scales of motion. In the k-ε standard model, the eddy viscosity is determined from a single turbulence length scale, while all the scales of motion contribute to the turbulent diffusion. Accordingly, in rapidly strained flows, the RNG model yields a lower turbulent viscosity than the k-ε standard. As a consequence, the RNG model more properly accounts for the effects of rapid strain and streamline curvature than the k-ε standard model, which explains the higher performance of the RNG model for some types of flows (i.e. rotating jets). Finally, the k-ε standard model has been shown to be unable to correctly reproduce the evolution of turbulent parameters, especially at high Reynolds numbers and rotating jets (like in the case of high swirl or tumble), which sometimes leads to the incorrect prediction of the mixture stratification in DI engines [14].

In addition to the RNG variant, the realizable k-ε model is considered in this paper. It has shown better accuracy than the k-ε standard model under some flow conditions. An extra advantage of using the realizable k-ε model implemented in Fluent is that it allows tuning the turbulent Schmidt number, S_c. Since S_c affects fuel dispersion, a parametric study of this number is also performed with the goal of overcoming the under-prediction in fuel dispersion by the RNG k-ε model, as shown in previous work [18,19].

RESULTS AND DISCUSSION

As previously mentioned, the proposed numerical approach aims at describing the whole engine working cycle, including the gas-exchange phase, in order to take the real conditions in terms of flow-field prior to hydrogen high-pressure direct injection into account. Results on the numerical predictions of the flow field at IVC are already available in literature [19] and will only be briefly discussed here. Figure 3 shows the comparison between experimental and numerical data in terms of velocity magnitude at IVC (−140°CA).

Overall, the agreement between simulation and experiments is satisfactory, despite a discrepancy in terms of location of vortex centers, which corresponds to the diagonally-upward motion of the charge in the numerical results, whereas the flow is perfectly vertical in the experimental results. Computational grids characterized by higher resolution were also tested in the simulations of the gas-exchange process, nevertheless the quality of numerical results did not improve and differences between numerical and experimental data in terms of in-cylinder flow persisted. However, these differences are relatively minor. A crude estimate, which assumes that the charge motion throughout the entire volume of the cylinder can be represented by the velocity field in the

THIS DOCUMENT IS PROTECTED BY U.S. COPYRIGHT
It may not be reproduced, stored in a retrieval system, distributed or transmitted, in whole or in part, in any form or by any means.
Downloaded from SAE International by Argonne National Laboratory, Copyright 2011 SAE International
Monday, November 07, 2011 12:11:32 PM

Table 2. Main characteristics of the analyzed computational grids

	Mesh 1	Mesh 2	Mesh3
Total number of cells (at BDC)	200,000	1,400,000	3,300,000
Cells in the nozzle domain	500	3,500	6,000
Cells across the nozzle diameter	4	8	10
Cell size in the nozzle (mm)	0.365	0.182	0.146
8-cores simulation time (hours)	≈2	≈10	≈16

central symmetry plane, yields that the momentum introduced by the injection event (at critical conditions in the nozzle) is about 9.5 times higher than that of the bulk gas. Hence post-injection deviations of simulation and experiment cannot be attributed to inaccuracies in the prediction of the pre-injection flow. Indeed, recent work [34] shows that an increase of the pre-injection tumble ratio by a factor of 4 is needed to yield significant changes in the post-injection convection of the fuel cloud. Starting from the IVC, the present analysis focuses on the mixture formation process and on the influence of geometrical (grid resolution) and physical (turbulence model) settings on the quality of the numerical results.

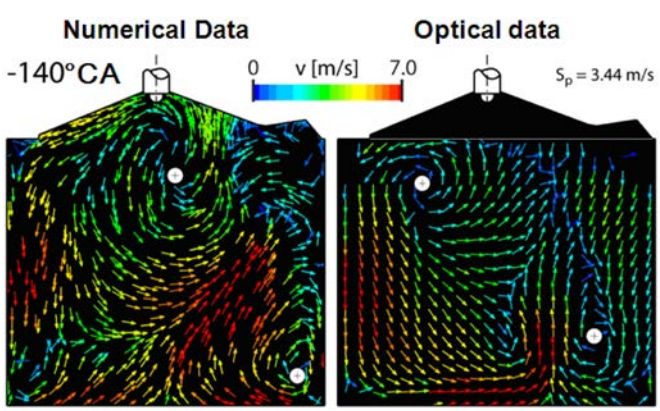

Figure 3. Numerical (left) and experimental (right) in-cylinder velocity field at IVC [19]

INFLUENCE OF GRID RESOLUTION

The main characteristics of the three computational grids used in this study are reported in Table 2. The grid resolution, in the overall as well as near-nozzle domain, has been progressively increased from 200,000 to over 3,000,000 cells. Simulations have been performed in parallel on 8 cores and even for the finest mesh computational times are affordable. Figure 4 shows the three grids in detail. In particular, the significant increase in the number of cells along the nozzle diameter can be noticed.

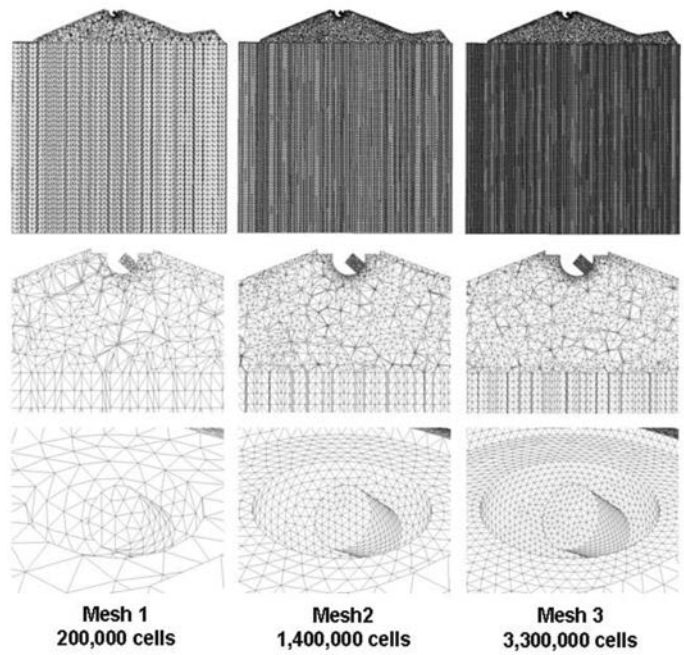

Figure 4. Overall and near-nozzle resolution of the used computational grids

In general, all three grids are able to provide expected results for the under-expanded jets (Figure 5), with Mach numbers close to unity in the nozzle volume and greater than unity immediately after the nozzle critical section. The maximum jet velocity in the under-expanded region reaches values above 2000 m/s, much higher than the speed of sound in the nozzle (≈1250 m/s), which depends on fluid properties and jet temperature (set to 300K in the inlet boundary conditions). The coarse grid (Mesh 1) shows a smaller region where the jet is under-expanded and higher jet diffusion. This is consistent with the results in terms of jet penetration. In general, a fine grid tends to increase the turbulent transport of the physical and chemical quantities along the jet direction. Even though the physics relevant to under-expansion of gaseous jets is not the major focus of this work, the authors acknowledge that the approach here proposed is not completely able to describe typical phenomena (barrel and

THIS DOCUMENT IS PROTECTED BY U.S. COPYRIGHT
It may not be reproduced, stored in a retrieval system, distributed or transmitted, in whole or in part, in any form or by any means.
Downloaded from SAE International by Argonne National Laboratory, Copyright 2011 SAE International
Monday, November 07, 2011 12:11:32 PM

reflected shock) of the under-expanded region. A higher level of detail may be gained by increasing mesh resolution and employing structured grids in the near-nozzle domain.

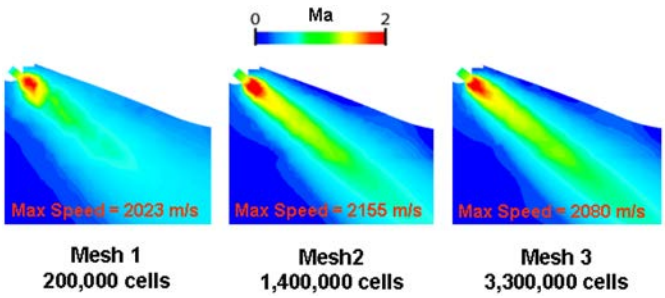

Figure 5. Mach number in the under-expanded jet region for the three grids here analyzed

Figure 6 shows the effect of grid resolution on the numerical results and compares numerical and optical data in terms of hydrogen mole-fraction. The k-ε RNG model is used for this analysis. Results show that a coarse grid is not able to provide an accurate prediction of the jet penetration. At −130°CA, with a coarse mesh, the jet has just hit the cylinder wall, while it has almost reached the piston with the two finer grids. This difference is mainly due to the grid resolution in the nozzle and near-nozzle region, which significantly influences the jet penetration. The overall resolution might also affect the jet penetration and shape, with particular regard to jet-wall interaction.

After end of injection, no noticeable effects of grid resolution on air entrainment in the jet are visible except in a small region near the pent-roof where part of the fuel jet re-circulates after impinging on the walls. At this location, it appears that the coarse mesh has insufficient grid resolution near the wall, and too much fuel is trapped in the intake quenching zone. This phenomenon may also be related to the crude modeling of the injection transients as linear ramp-up and ramp-down. Currently, the real transient behavior of the injector is unknown, however the authors intend to investigate more suitable modeling of start and end of injection by means of the comparison with high-speed Schlieren imaging.

Beyond 1,400,000 cells, further reduction of cell size does not show noticeable changes in the predicted fuel distribution. Figure 6 shows that numerical results for 1,400,000 cells and 3,300,000 cells are almost identical. Accordingly, further increasing the grid resolution most likely will not provide a better agreement with experiments.

Thus, the main findings of this parametric study can be summarized as follows:

• Grid resolution strongly influences the jet penetration, while it has almost no effect on the fuel dispersion, which is under-predicted at every resolution.

• The resolution in the near-nozzle region is the dominating factor for jet penetration. The overall and near-wall cell size have a secondary but not negligible effect.

• Numerical results reported here and later in this paper are grid-independent, beyond 1.4 millions of cells at BDC.

The numerical simulation of a single jet does not have to face a typical issue affecting multi-hole nozzles, the Coanda effect (i.e. several jets merge into a single jet). Preliminary analysis has shown that grid independence at the current resolution may not hold for more complicated geometries that have jet-jet interaction. Corresponding investigations are in progress.

In this paper, neither the required wall-treatment, nor the optimum cells size at the wall boundaries, has been investigated to model the jet-wall interaction. Uniform grids and the standard wall functions option have been used and the comparison between numerical and experimental data has shown a good agreement in terms of wall-jet interaction. Nevertheless in Figure 6, between −130°CA and −110°CA, it is possible to notice that experimentally the jet detaches from the walls more than in the numerical results and that the fuel concentration increases (compared to the numerical data) in the orthogonal direction with respect to the wall surface. This indicates that additional accuracy may be gained from improving the wall treatment.

On the other hand, experimental uncertainties may affect the conversion of acetone fluorescence into actual H2 mole-fraction value. As an example, the slightly elevated fuel mole-fraction that the experiment measures near the wall at −130°CA and −120°CA is likely to be an experimental inaccuracy. The fluorescence signal measured in the experiment is related to the fuel mole-fraction, shown here, via the assumption of constant pressure throughout the field of view. Strong deceleration of the jet near the wall would locally increase pressure, which would be (incorrectly) interpreted as increased mole fraction.

INFLUENCE OF TURBULENCE MODEL

The previous parametric analysis shows that the grid resolution has a limited effect on the agreement between modeling and experiments. In particular, it affects the jet penetration but does not seem to influence the fuel dispersion. Figure 6 shows that the fuel concentration gradients in the optical data are smoother than in the numerical data. A previous study [19] has also shown that, when the piston approaches TDC, the dissipation of the tumble motion in the numerical results is much slower than in the experiments. One of the hypotheses that the authors have made is that the

THIS DOCUMENT IS PROTECTED BY U.S. COPYRIGHT
It may not be reproduced, stored in a retrieval system, distributed or transmitted, in whole or in part, in any form or by any means.
Downloaded from SAE International by Argonne National Laboratory, Copyright 2011 SAE International
Monday, November 07, 2011 12:11:32 PM

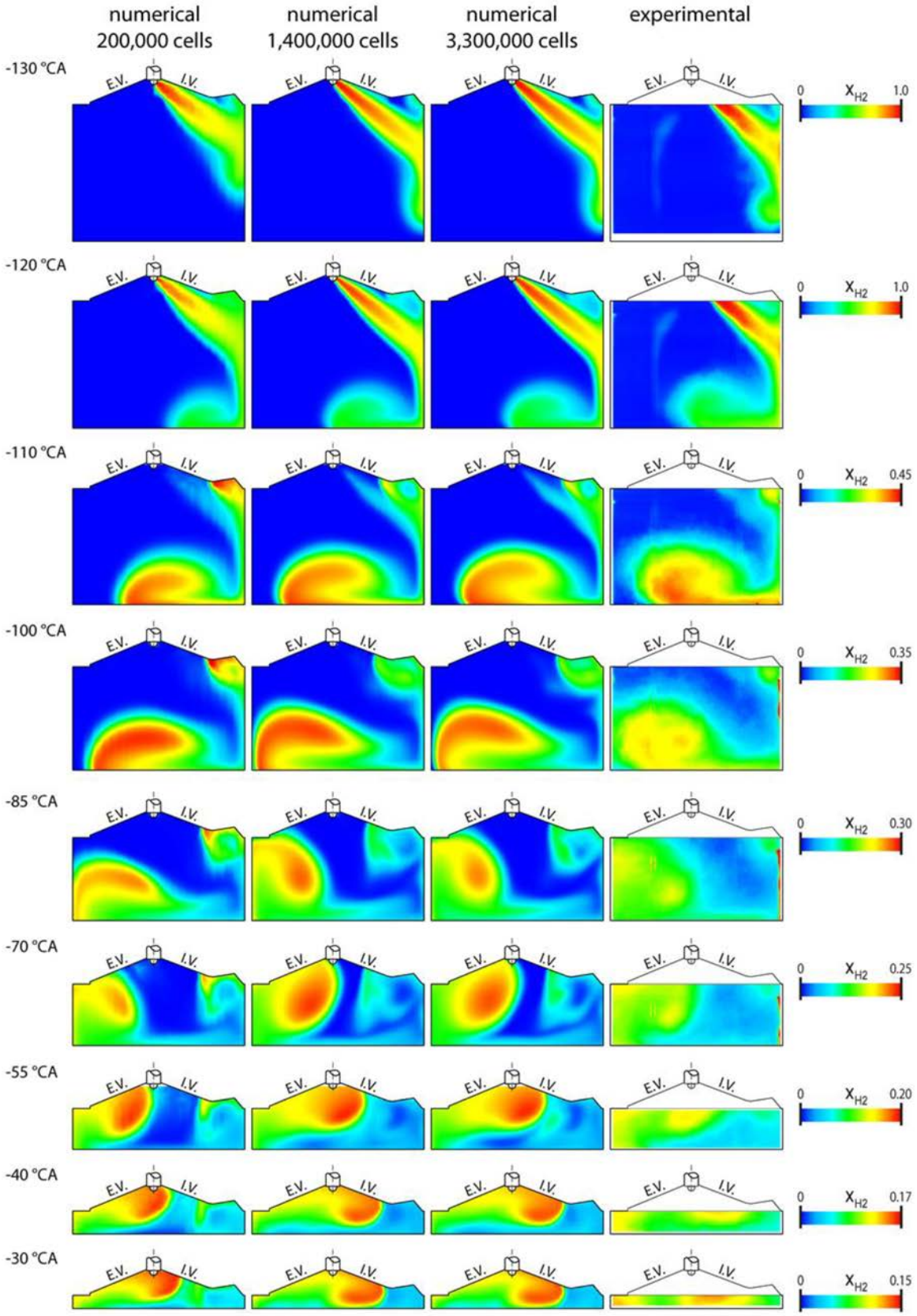

Figure 6. Hydrogen mole-fraction during the compression stroke: Comparison between numerical and optical data and influence of the grid resolution (k-ε RNG model)

THIS DOCUMENT IS PROTECTED BY U.S. COPYRIGHT
It may not be reproduced, stored in a retrieval system, distributed or transmitted, in whole or in part, in any form or by any means.
Downloaded from SAE International by Argonne National Laboratory, Copyright 2011 SAE International
Monday, November 07, 2011 12:11:32 PM

turbulence model is not able to correctly predict the dissipation of the turbulent energy and in particular the turbulent energy transfer from the largest to the smallest turbulent scales.

A preliminary analysis of the three versions of the k-ε model (standard, RNG and realizable) implemented in the Fluent solver showed no significant differences. The RNG and realizable versions have provided very similar results and are commonly considered more suitable than the standard k-ε to describe rotating jets, like in this study. Therefore, the k-ε realizable model, which allows modification of the default value of the turbulent Schmidt number, was used to tune the turbulence model. The turbulent Schmidt number, as defined by Equation 1:

$$Sc_t = \nu_t / D_t \tag{1}$$

represents the ratio between the turbulent kinematic viscosity ν_t and the turbulent coefficient of molecular diffusion D_t. Accordingly, reducing the Schmidt number means increasing the molecular diffusion over the jet viscosity and consequently increasing the fuel dispersion over convection. The default setting in the Fluent solver is S_c = 0.7, nevertheless in many CFD applications, S_c generally varies in the range of 0.2 to 1.3. In this paper, S_c is set to 0.7, 0.55 and 0.2. Figure 7 shows the numerical results obtained by two different versions of the k-ε model (RNG and realizable), with two attempts of "tuning" of the k-ε realizable model. In all the cases, the computational grid consists of 1,400,000 cells (at BDC) and the optical data is also shown for comparison.

It can be observed that the k-ε realizable model provides a richer hydrogen cloud in the jet core and increased fuel dispersion at the jet boundaries (−85°CA), even if the final mixture stratification is very similar to the one predicted by the k-ε RNG. A better comparison of numerical and experimental data is currently not feasible, due to the lack of optical data in the pent-roof. Nevertheless, the realizable as well as the RNG version of the k-ε model predict a richer zone within the fuel jet which is located below the intake valve at −30°CA. The realizable formulation provides smoother gradients along the jet and tends to yield better agreement with the measured H2 mole-fraction values at late crank angles. However, even employing the realizable version of the k-ε model, at earlier crank angles (from −100°CA up to −55°CA) the difference between experiments and modeling in term of concentration gradients is still remarkable.

As the turbulent Schmidt number is reduced, first to S_c = 0.55 and then to S_c =0.2, a better fuel dispersion is expected. Figure 7 shows that, although numerical results for S_c = 0.2 provide a better match with optical data at some crank angles (from −70°CA to −40°CA), at −30°CA it is not possible to identify rich and lean zones within the hydrogen cloud anymore. Also, the tuning does not seem to significantly improve the agreement between numerical and experimental data during the early compression.

In summary, these are the main results of this parametric study:

• The choice of turbulence model and the tuning of fuel dispersion do not influence the jet penetration and overall evolution throughout the cylinder.

• The realizable version of the k-ε model shows a slight increase in fuel dispersion when compared to the RNG formulation.

• Tuning (reduction) of the turbulent Schmidt number allows for a further increase of fuel dispersion. Nevertheless, the model starts losing the information on where relatively rich and lean zones are located within the jet cloud, especially for late crank angles.

CONCLUSIONS

Direct injection is a promising strategy to meet the target set for H2 ICES by the U.S. Department of Energy in terms of engine efficiency, NOX emissions and power density. The main challenge for a DI strategy is the need for a proper setup in order to optimize the mixture formation process. Numerical simulation can be used as an effective diagnostic and development tool but needs to be carefully validated and, to this aim, experimental data from an optically accessible engine are of crucial importance.

This paper reports a parametric analysis of the influence of grid resolution and turbulence model on the numerical results in terms of fuel concentration in a DI-H2 ICE. Gaseous hydrogen is injected from a high-pressure (100 bar) injector with a single-hole nozzle providing a supersonic jet. Simulations account for the in-cylinder flow prior to fuel injection, which is overall well predicted.

The grid resolution is found to have significant influence on jet penetration. Numerical results presented for a 1,400,000 cells computational mesh are grid-independent and finer grids do not provide any improvement in the current prediction. The grid resolution has no effect on the fuel dispersion, which is under-predicted at every resolution.

The turbulent models and their settings do not have any influence on jet penetration. However, there are improvements in terms of fuel dispersion which need further optimization. In particular, the realizable version of the k-ε model shows a slight increase in fuel dispersion and slightly

THIS DOCUMENT IS PROTECTED BY U.S. COPYRIGHT
It may not be reproduced, stored in a retrieval system, distributed or transmitted, in whole or in part, in any form or by any means.
Downloaded from SAE International by Argonne National Laboratory, Copyright 2011 SAE International
Monday, November 07, 2011 12:11:32 PM

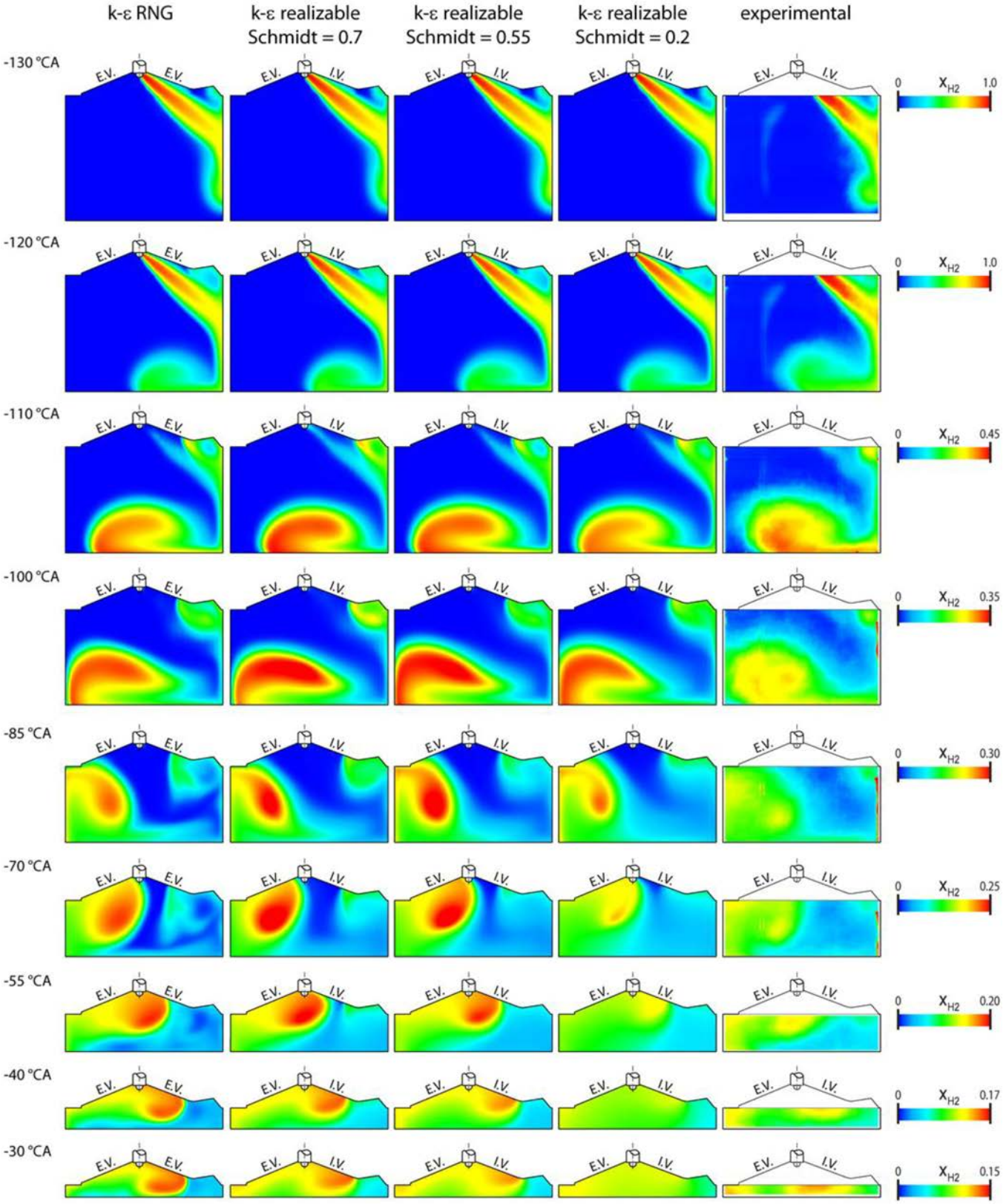

Figure 7. Hydrogen mole-fraction during the compression stroke: Comparison between numerical and optical data and influence of the turbulence model (grid resolution = 1,400,000 cells at BBC)

THIS DOCUMENT IS PROTECTED BY U.S. COPYRIGHT
It may not be reproduced, stored in a retrieval system, distributed or transmitted, in whole or in part, in any form or by any means.
Downloaded from SAE International by Argonne National Laboratory, Copyright 2011 SAE International
Monday, November 07, 2011 12:11:32 PM

better agreement with optical data, when compared to the RNG formulation.

Finally, the comparison between numerical and experimental data shows a remarkable agreement in terms of jet penetration, wall impingement and overall evolution. Predictions of fuel dispersion need to be improved. Higher level of detail in the wall treatment is currently under investigation as well as experimental inaccuracies in the PLIF measurements. Nevertheless, the described numerical model shows a significant predictive capability and can already be utilized as a powerful tool for engine efficiency optimization.

ACKNOWLEDGMENTS

This manuscript has been created by UChicago Argonne, LLC, Operator of Argonne National Laboratory ("Argonne") and Sandia National Laboratories ("Sandia"). Argonne, a U.S. Department of Energy Office of Science laboratory, is operated under Contract No. DE-AC02-06CH11357. Sandia is a multiprogram laboratory operated by Sandia Corporation, a Lockheed Martin Company, for the United States Department of Energy's National Nuclear Security Administration under contract DE-AC04-94AL85000. The U.S. Government retains for itself, and others acting on its behalf, a paid-up nonexclusive, irrevocable worldwide license in said article to reproduce, prepare derivative works, distribute copies to the public, and perform publicly and display publicly, by or on behalf of the Government.

The authors would like to thank especially Brad Boyer and Matt Younkins from Ford Motor Company for their invaluable support of the DI-H2ICE project. This research is funded by DOE's Vehicle Technologies Program, Office of Energy Efficiency and Renewable Energy, with Gurpreet Singh as the program manager.

REFERENCES

1. Verhelst, S., Sierens, R., and Verstraeten, S., "A Critical Review of Experimental Research on Hydrogen Fueled SI Engines," SAE Technical Paper 2006-01-0430, 2006, doi: 10.4271/2006-01-0430.

2. Verhelst, S., Wallner, T., Hydrogen-fueled internal combustion engines, Progress in Energy and Combustion Science, Volume 35, Issue 6, December 2009, Pages 490-527, 2009.

3. White, C.M., Steeper, R. R., Lutz, A. E., The hydrogen-fueled internal combustion engine: a technical review. Int. J. Hydrogen Energy 31:1292-1305, 2006.

4. U.S. Department of Energy, FreedomCAR and Fuel Technical Partnership Technical Goals, Washington, D.C., 2002.

5. Wallner, T., Nande, A., and Naber, J., "Evaluation of Injector Location and Nozzle Design in a Direct-Injection Hydrogen Research Engine," SAE Technical Paper 2008-01-1785, 2008, doi:10.4271/2008-01-1785.

6. Wallner, T., Nande, A., and Naber, J., "Study of Basic Injection Configurations using a Direct-Injection Hydrogen Research Engine," *SAE Int. J. Engines* **2**(1):1221-1230, 2009, doi:10.4271/2009-01-1418.

7. Wallner, T., Scarcelli, R., Nande, A., and Naber, J., "Assessment of Multiple Injection Strategies in a Direct-Injection Hydrogen Research Engine," *SAE Int. J. Engines* 2(1):1701-1709, 2009, doi:10.4271/2009-01-1920.

8. Nande, A., Wallner, T., and Naber, J., "Influence of Water Injection on Performance and Emissions of a Direct-Injection Hydrogen Research Engine," SAE Technical Paper 2008-01-2377, 2008, doi:10.4271/2008-01-2377.

9. Wallner, T., Nande, A., Scarcelli, R., Evaluation of exhaust gas recirculation (EGR) in combination with direct injection (DI) on a Hydrogen Research Engine, presented at World Hydrogen Technology Convention, New Delhi/India, 2009.

10. Wimmer, A., Wallner, T., Ringler, J., and Gerbig, F., "H2-Direct Injection - A Highly Promising Combustion Concept," SAE Technical Paper 2005-01-0108, 2005, doi: 10.4271/2005-01-0108.

11. Obermair, H., Scarcelli, R., and Wallner, T., "Efficiency Improved Combustion System for Hydrogen Direct Injection Operation," SAE Technical Paper 2010-01-2170, 2010, doi: 10.4271/2010-01-2170.

12. Tanno, S., Ito, Y., Michikawauchi, R., Nakamura, M. et al., "High-Efficiency and Low-NOx Hydrogen Combustion by High Pressure Direct Injection," *SAE Int. J. Engines* **3**(2): 259-268, 2010, doi:10.4271/2010-01-2173.

13. Messner, D., Wimmer, A., Gerke, U., and Gerbig, F., "Application and Validation of the 3D CFD Method for a Hydrogen Fueled IC Engine with Internal Mixture Formation," SAE Technical Paper 2006-01-0448, 2006, doi: 10.4271/2006-01-0448.

14. Heindl, R., Eichlseder, H., Spuller, C., Gerbig, F. et al., "New and Innovative Combustion Systems for the H2-ICE: Compression Ignition and Combined Processes," *SAE Int. J. Engines* **2**(1):1231-1250, 2009, doi:10.4271/2009-01-1421.

15. Salazar, V. and Kaiser, S., "An Optical Study of Mixture Preparation in a Hydrogen-fueled Engine with Direct Injection Using Different Nozzle Designs," *SAE Int. J. Engines* **2**(2):119-131, 2009, doi:10.4271/2009-01-2682.

16. Kaiser, S. and White, C., "PIV and PLIF to Evaluate Mixture Formation in a Direct-Injection Hydrogen-Fuelled Engine," *SAE Int. J. Engines* **1**(1):657-668, 2008, doi: 10.4271/2008-01-1034.

17. Salazar, V. and Kaiser, S., "Influence of the In-Cylinder Flow Field (Tumble) on the Fuel Distribution in a DI

THIS DOCUMENT IS PROTECTED BY U.S. COPYRIGHT
It may not be reproduced, stored in a retrieval system, distributed or transmitted, in whole or in part, in any form or by any means.
Downloaded from SAE International by Argonne National Laboratory, Copyright 2011 SAE International
Monday, November 07, 2011 12:11:32 PM

Hydrogen Engine Using a Single-Hole Injector," *SAE Int. J. Engines* **3**(1):309-325, 2010, doi:10.4271/2010-01-0579.

18. Scarcelli, R., Wallner, T., Salazar, V., and Kaiser, S., "Modeling and Experiments on Mixture Formation in a Hydrogen Direct-Injection Research Engine," *SAE Int. J. Engines* **2**(2):530-541, 2009, doi:10.4271/2009-24-0083.

19. Scarcelli, R., Wallner, T., Salazar, V.M., Kaiser, S.A., "CFD and Optical Investigations of Fluid Dynamics and Mixture Formation in a DI-H2 ICE", ASME ICEF Conference 2010 (San Antonio, Texas, USA), ASME Paper ICEF2010-35084, 2010.

20. Salazar, V., Kaiser, S., and Halter, F., "Optimizing Precision and Accuracy of Quantitative PLIF of Acetone as a Tracer for Hydrogen Fuel," *SAE Int. J. Fuels Lubr.* **2**(1): 737-761, 2009, doi:10.4271/2009-01-1534.

21. Thurber, M. C., Grisch, F., Kirby, B. J., Votsmeier, M., Hanson, R. K., Measurements and Modeling of Acetone Laser-Induced Fluorescence with Implications for Temperature-Imaging Diagnostics, Appl. Optics 37 (1998) 4963-4978, 1998.

22. Thurber, M. C., Hanson, R. K., Pressure and composition dependences of acetone laser-induced fluorescence with excitation at 248, 266, and 308 nm, Appl. Phys. B - Lasers Opt. 69 (1999) 229-240.

23. Espey, C., Dec, J. E., Litzinger, T. A., Santavicca, D. A., Planar laser rayleigh scattering for quantitative vapor-fuel imaging in a diesel jet, Combust. Flame 109 (1997) 65-86, 1997.

24. Hwang, W., Dec, J., and Sjöberg, M., "Fuel Stratification for Low-Load HCCI Combustion: Performance & Fuel-PLIF Measurements," SAE Technical Paper 2007-01-4130, 2007, doi:10.4271/2007-01-4130.

25. Yeh, C., Kamimoto, T., Kosaka, H., and Kobori, S., "Quantitative Measurement of 2-D Fuel Vapor Concentration in a Transient Spray via Laser-Induced Fluorescence Technique," SAE Technical Paper 941953, 1994, doi: 10.4271/941953.

26. Abraham, J., "What is Adequate Resolution in the Numerical Computations of Transient Jets?," SAE Technical Paper 970051, 1997, doi: 10.4271/970051.

27. Andreassi, L., Facci, A.L., Ubertini, S. "Numerical simulation of gaseous fuel injection: A new methodology for multi-dimensional modeling", Int. J. Numer. Meth. Fluids 2010; 64:609-626, 2010.

28. Andreassi, L., Facci, A.L., Krastev, V.K., Ubertini, S. "Multidimensional modelling of gaseous injection: Analysis of an impinging jet", Int. J. Heat and Fluid Flow, Vol. 31, Issue 5, 909-915, 2010.

29. Hessel, R., Abani, N., Aceves, S., and Flowers, D., "Gaseous Fuel Injection Modeling Using a Gaseous Sphere Injection Methodology," SAE Technical Paper 2006-01-3265, 2006, doi:10.4271/2006-01-3265.

30. Whitesides, R., Hessel, R.P., Flowers, D., Aceves, S.M., "Application of Gaseous Sphere Injection Model for Modeling Under-expanded H2 Injection", presented at 33rd International Symposium on Combustion, Beijing, China, 2010.

31. Andreassi, L., Facci, A.L., Ubertini, S. "Three-Dimensional Simulation of Gaseous Fuel Injection Through a Hybrid Approach", J. Eng. Gas Turbines Power, Vol. 132, Issue 7, 2010.

32. Sukumaranan, S., Kong, S.C., "Numerical study on mixture formation characteristics in a direct-injection hydrogen engine", Int. J. hydrogen energy 35, 7991-8007, 2010.

33. Baratta, M., Catania, A.E., Pesce, F.C. "Computational and Experimental Analysis of Direct CNG Injection and Mixture Formation in a Spark Ignition Research Engine" ASME ICEF Conference 2010 (San Antonio, Texas, USA), ASME Paper ICEF2010-35103, 2010.

34. Salazar, V. and Kaiser, S., "Interaction of Intake-Induced Flow and Injection Jet in a Direct-Injection Hydrogen-Fueled Engine Measured by PIV," SAE Technical Paper 2011-01-0673, 2011, doi:10.4271/2011-01-0673.

ABBREVIATIONS

ATDC
After Top Dead Center

BDC
Bottom Dead Center

BTDC
Before Top Dead enter

BTE
Brake Thermal Efficiency

°CA
Degree Crank Angle

CCD
Charge-Coupled Device

CFD
Computational Fluid Dynamics

CNG
Compressed Natural Gas

THIS DOCUMENT IS PROTECTED BY U.S. COPYRIGHT
It may not be reproduced, stored in a retrieval system, distributed or transmitted, in whole or in part, in any form or by any means.
Downloaded from SAE International by Argonne National Laboratory, Copyright 2011 SAE International
Monday, November 07, 2011 12:11:32 PM

CO2
Carbon Dioxide

DI
Direct Injection

DNS
Direct Numerical Simulation

EVO
Exhaust Valve Opening

EOI
End of injection

H2
Hydrogen

ICE
Internal Combustion Engine

IMEP
Indicated Mean Effective Pressure

IVC
Intake Valve Closing

LES
Large Eddy Simulation

N2
Nitrogen

Nd:YAG
Neodymium-doped Yttrium Aluminum Garnet

NOX
Nitrogen Oxides

PFI
Port Fuel Injection

PIV
Particle Image Velocimetry

PLIF
Planar Laser-Induced Fluorescence

RANS
Reynolds-Averaged Navier-Stokes

RNG
Renormalization Group

RPM
Revolution per Minute

SOI
Start of Injection

TDC
Top Dead Center

CONTACT INFORMATION

Riccardo Scarcelli, Ph.D.
Argonne National Laboratory
Energy Systems Division
Building 362
9700 South Cass Avenue
Argonne, IL 60439-4815
www.anl.gov
Phone: 630.252.6940
Fax: 630.252.3443
rscarcelli@anl.gov

THIS DOCUMENT IS PROTECTED BY U.S. COPYRIGHT
It may not be reproduced, stored in a retrieval system, distributed or transmitted, in whole or in part, in any form or by any means.
Downloaded from SAE International by Argonne National Laboratory, Copyright 2011 SAE International
Monday, November 07, 2011 12:11:32 PM

The Engineering Meetings Board has approved this paper for publication. It has successfully completed SAE's peer review process under the supervision of the session organizer. This process requires a minimum of three (3) reviews by industry experts.

All rights reserved. No part of this publication may be reproduced, stored in a retrieval system, or transmitted, in any form or by any means, electronic, mechanical, photocopying, recording, or otherwise, without the prior written permission of SAE.

ISSN 0148-7191

Positions and opinions advanced in this paper are those of the author(s) and not necessarily those of SAE. The author is solely responsible for the content of the paper.

SAE Customer Service:
Tel: 877-606-7323 (inside USA and Canada)
Tel: 724-776-4970 (outside USA)
Fax: 724-776-0790
Email: CustomerService@sae.org
SAE Web Address: http://www.sae.org
Printed in USA